# Stationary States of External Cavity Diode Laser

V.Z.Tronciu
Department of Physics, Technical University of Moldova
Chisinau, Republic of Moldova
tronciu@mail.utm.md

M.Radziunas
Weierstrass Institute, Berlin
Mohrenstraße 39, 10117 Berlin, Germany

H.Wenzel
Ferdinand-Braun-Institut, Leibniz-Institut für Höchstfrequenztechnik
Gustav-Kirchhoff Str. 4, 12489 Berlin, Germany

***Abstract* — We report the results of numerical investigations of the stationary states of an external cavity diode laser (ECDL) device composed of a semiconductor laser, a lens, and a distant Bragg grating, which provides optical feedback. A rate equation model was used to simulate and analyze the behavior of the considered laser device.**

***Key Words* — optical feedback, semiconductor lasers, bifurcations, external cavity modes.**

## I. Introduction

During recent years the control and stabilization of the emission of semiconductor lasers by an external cavity has received considerable attention. In particular, wavelength stabilized, narrow-spectral linewidth semiconductor lasers are required for different applications such as frequency conversion, quantum optical experiments, coherent optical communications, spectroscopy etc. Wavelength stabilization can be achieved by the integration of a Bragg grating into the resonator, either monolithically into the laser chip (distributed feedback laser, distributed Bragg reflector laser) or in an external cavity configuration [1].

The simplest method for the modelling of a semiconductor laser with a weak optical feedback is given by the Lang-Kobayashi (LK) model [2]. The LK modelling approach can be used to get a deeper understanding of the stabilization or destabilization of the stationary states of external cavity lasers (ECDLs). In the present paper the LK model is used for a numerical investigation of the stationary states of a ECDL composed of an amplifying semiconductor section, a lens and a distant Bragg grating that provides optical feedback. The paper is organized as follows. The device structure and mathematical model are described in Section II. Section III presents the related numerical and experimental results. Finally, some conclusions are given in Section IV.

## II. Model And Equations

The investigated ECDL is schematically shown in Fig. 1. It consists of a semiconductor laser coupled to an external holographic Bragg grating providing spectrally filtered optical feedback. Additional feedback is provided by a lens located between laser chip and Bragg grating. The laser dynamics is analyzed using an extended Lang-Kobayashi rate equation model [2] appropriate for filtered feedback [3] for the complex field amplitudes E(t) and F(t) and the excess carrier density N(t),

$$\frac{dE(t)}{dt}=(1+i\alpha)\left[g_N(N(t)-N_0)-\frac{1}{\tau_{ph}}\right]\frac{E(t)}{2} + \gamma_1 e^{i\varphi}E(t-\tau_1)+\gamma_2 F(t) \quad (1)$$

$$\frac{dN(t)}{dt}=\frac{I}{q}-\frac{N(t)}{\tau_e}-g_N(N(t)-N_0)\,|E(t)|^2, \quad (2)$$

$$\frac{dF(t)}{dt}=\lambda E(t-\tau_2)e^{i\psi}+(i\Delta\omega-\lambda)F(t), \quad (3)$$

where $\tau_1$, $\tau_2$ are the roundtrip times in the cavities between laser chip and lens and between laser and Bragg grating, respectively and $\varphi = \omega_0\tau_1$, $\psi = \omega_0\tau_2$ are the corresponding accumulated optical phases. $\gamma_1$ and $\gamma_2$ are the feedback strengths governed by the reflectivity's $R_1$ of the lens and $R_2$ of the Bragg grating, respectively. $I$ is the injection current. The other parameter values are: $\alpha$ = 1.8 is the linewidth enhancement factor, $g$ = 1.5x10$^5$ ns$^{-1}$ is the differential gain, $\tau_{ph}$ = 2 ps and $\tau_e$ = 1 ns are the photon and carrier lifetimes, respectively; $N_0$ = 1.5x10$^8$ is the carrier number at the transparency.

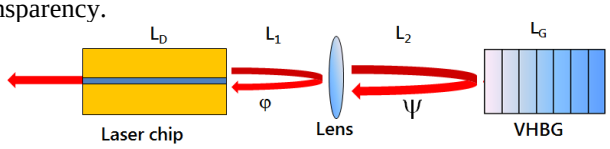


Fig. 1. Laser setup.

The stationary states of equations (1)-(3) known as external cavity modes (ECMs) are given by solutions with the following form:

$$E(t)=E_s\cdot e^{i\omega_s t},\ F(t)=F_s\cdot e^{i\omega_s t+i\Phi_s},\ N(t)=N_s \quad (4)$$

where $E_s$, $F_s$, $N_s$ are time-independent real constants. Inserting (4) into (1)-(3) and separating the real and imaginary parts we obtain a transcendental equation for $\omega_s$

$$\omega_s=\gamma_1\sqrt{1+\alpha^2}\sin\left(\varphi-\omega_s\tau_1-\arctan(\alpha)\right)+ +\frac{\gamma_2\sqrt{1+\alpha^2}}{\sqrt{1+\delta^2}}\sin\left(\psi-\omega_s\tau_2-\arctan(\alpha)-\arctan(\delta)\right) \quad (5)$$

where $\delta=(\omega_s-\Delta\omega)/\lambda$ [3].

## III. RESULTS

To understand the properties of the laser under the influence of filtered feedback, we consider the laser dynamics in terms of bifurcation diagrams as shown in Fig. 2. Figure 2 (left) shows the calculated maximum (black) and minimum (red) photon numbers versus feedback strength $\gamma_2$. As the feedback strength is increased from zero, first CW operation is observed and the corresponding photon number is given by a solid line. At a certain feedback strength, denoted by H in the figure, there is a Hopf bifurcation and the laser begins to pulsate. The Hopf bifurcation is supercritical and, as expected, the oscillation amplitude grows with the square root of the distance from the bifurcation point. The line P gives the peak photon number in the pulsation or periodic regime. As the feedback strength is increased further, a scenario compatible with the quasiperiodic route to chaos is obtained and several instabilities take place.

When the feedback strength reaches the value $\gamma_2 = 27$ ns$^{-1}$, a jump back to a CW operation region is observed. For values of the feedback strength 17 ns$^{-1}$ < $\gamma_2$ < 27 ns$^{-1}$ the system displays a chaotic behavior. Figure 2 (right) displays the bifurcation diagram for the feedback phase acting as bifurcation parameter. Let us, e.g., consider the case that the phase φ is increased. For low values of the feedback phase φ the dynamics of the laser is chaotic. It can be noticed from the figure that the amplitude of the chaotic oscillations slightly decreases with the increase of the phase terminated by the periodic solution (see Fig. 2). The CW states are within the Hopf bifurcations denoted by H.

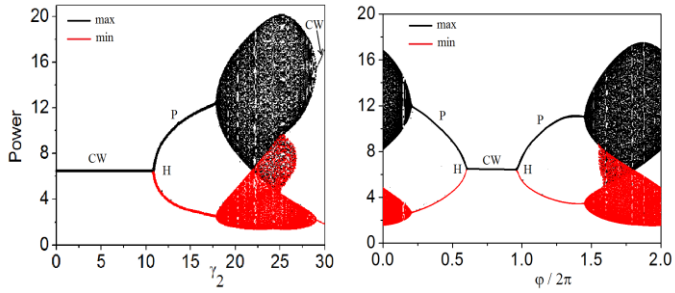


Fig. 2. Numerical bifurcation diagrams for feedback strength $\gamma_2$ (left) and phase φ (right) being bifurcation parameters. 'CW' denotes continuous-wave operation, 'H' Hopf bifurcation and 'P' stable periodic solution.

So far we have clarified different aspects of laser bifurcations under the influence of feedback. In what follows, we focus on the stationary solutions (so called external cavity modes, ECMs) of equations (1) - (3) presented in the form (5). It is well known that in the case of conventional optical feedback the ECMs are located on ellipses if the air gap phase is varied between 0 and 2π. For feedback strengths smaller than a critical value there is only one ECM. For feedback strengths above the critical value, larger numbers of ECMs appear. We mention that the ECMs appear and disappear in pairs (modes and anti-modes) at saddle-node bifurcations. Figure 3 shows the location of ECMs calculated using equation (5) for different values of the feedback strength. We first consider a small feedback strength $\gamma_1 = 5$ ns$^{-1}$, $\gamma_2 = 5$ ns$^{-1}$, where the location of the fixed points is similar to that of the conventional feedback case, i.e. the modes are located on an ellipse (see Fig. 3a). An increase of the feedback strength (see Figure 3b and 3d) results in the appearance of new satellite bubbles of ECMs on left and right hand sides of a deformed ellipse. The onset of these bubbles reflects the existence of frequency gaps for which no ECM solutions exist. These frequency gaps are originated from destructive interference in the feedback coming from the two cavities. When the feedback strengths are $\gamma_1 = 5$ ns$^{-1}$, $\gamma_2 = 20$ ns$^{-1}$ the feedback implies a non-elliptic location of modes (see Fig. 3c). This clearly illustrates that in the case of the two feedbacks, one from the lens and the other from the Bragg grating, the location of the modes becomes more complicated when compared with that of conventional feedback.

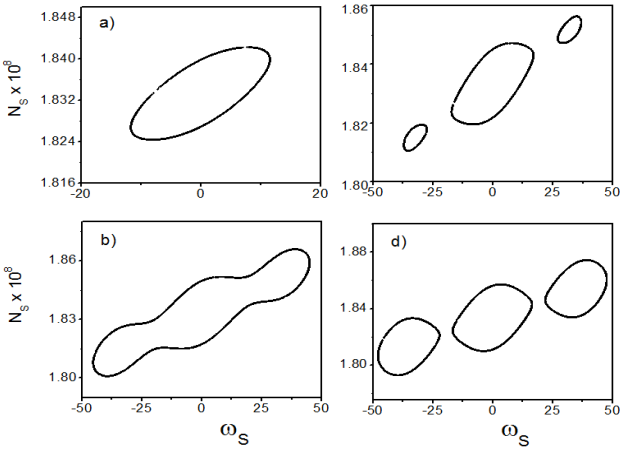


Fig. 3. Locus of the ECMs in the plane ($N_S$ - $\omega_S$) for different levels of feedback strength: a) $\gamma_1 = 5$ ns$^{-1}$, $\gamma_2 = 5$ ns$^{-1}$, b) $\gamma_1 = 5$ ns$^{-1}$, $\gamma_2 = 13$ ns$^{-1}$, c) $\gamma_1 = 5$ ns$^{-1}$, $\gamma_2 = 20$ ns$^{-1}$, and d) $\gamma_1 = 15$ ns$^{-1}$, $\gamma_2 = 20$ ns$^{-1}$, $\varphi$ and $\psi \in [0 \div 2\pi]$.

## CONCLUSIONS

In the framework of properly adapted Lang-Kobayashi equations, we have treated a single-mode semiconductor laser under the influence of optical feedback from a lens and a distant Bragg grating. Bifurcation diagrams in dependence of magnitude and phase of the feedback were calculated. An increase of the number of external cavity modes by rising feedback strength was shown.

## ACKNOWLEDGMENT

This work was supported by projects 11.817.05.17F and MANUMIEL (BMBFFKZ01DK13020A), STCU-5937, 5993.

## REFERENCES

[1] M. Radziunas, V.Z. Tronciu, E. Luvsandamdin, C. Kürbis, A. Wicht, and H. Wenzel Study of Microintegrated External-Cavity Diode Lasers: Simulations, Analysis, and Experiments, IEEE J. Quantum Electron., vol. 51, no. 2, 2000408 (2015).

[2] R. Lang and K. Kobayashi K. External optical feedback effects on semiconductor injection laser properties, IEEE J. Quantum Electron., vol. 16, pp. 347- 355. 1980

[3] I.V. Ermakov, V.Z. Tronciu, Pere Colet and C. Mirasso Controlling the unstable emission of a semiconductor laser subject to conventional optical feedback with a filtered feedback branch, Optics Express., vol. 17, p. 8749-8752009.